Electronic Processes in Conjugated Diblock Oligomers Mimicking Low Band-Gap Polymers: Experimental and Theoretical Spectral Analysis†

Jodi M. Szarko,[‡,§,∥] Brian S. Rolczynski,[‡,§,∥] Jianchang Guo,[§,∥,⊥] Yongye Liang,[⊥] Feng He,[⊥] Michael W. Mara,[‡,§,∥] Luping Yu,*[,⊥] and Lin X. Chen[‡,§,∥]

Department of Chemistry, Northwestern University, Evanston, Illinois 60208, Chemical Sciences and Engineering Division, Argonne National Laboratory, Argonne, Illinois 60439, Argonne-Northwestern Solar Energy Research (ANSER) Center, Northwestern University, 2145 Sheridan Road, Evanston, Illinois 60208, and Department of Chemistry and The James Franck Institute, The University of Chicago, 929 E 57th. Street, Chicago, Illinois, 60637

Received: March 3, 2010; Revised Manuscript Received: April 29, 2010

Conjugated oligomers containing a common central thienothiophene unit symmetrically connected to two identical thiophene oligomers were studied as model systems for a series of low bandgap organic diblock copolymers. The oligothiophene side chain fragments were varied in length as a means to tune the electronic coupling between the thienothiophene and oligothiophene moieties. The fragment length dependence of both the ground- and excited-state electronic and structural properties of a series of diblock oligomers were investigated in detail. The charge transfer character in these diblock oligomers, revealed by their optical absorption and fluorescence spectra, is responsible for their low band gap and energy gap tunability compared with their homooligomer counterparts. The electronic spectra and theoretical analysis indicate a partially localized central charge in the first excited state. Using experimental results and comparing them with theoretical calculations, we estimate that the electronic effects from a single thienothiophene unit spreads over seven to nine adjacent units through π-conjugation along the oligomers.

1. Introduction

The optical and electronic properties of organic conducting polymers and oligomers are very interesting and unique because they utilize an extensively delocalized π-electronic system. They are explored for potential applications in low-cost, easily processed, and lightweight devices, such as organic light-emitting diodes (OLEDs) and organic photovoltaic (OPV) devices.[1–4] In OPV devices, a conducting polymer is often used as the electron donor, whereas the electron acceptor is typically a molecule such as [6,6]-phenyl-C_{61}-butyric acid methyl ester (PCBM).[4] One of the most studied conducting polymers, poly-3-hexylthiophene (P3HT), has been used as a benchmark material because of its relatively high power conversion efficiency (PCE) compared with other conducting polymers.[5] Although device PCEs of >5% have been achieved using P3HT,[6] this value is still too low to make OPV materials a viable alternative for current commercial solar cell materials such as silicon.[7,8] OPV devices have a low PCE for several reasons: (1) inefficient light harvesting due to the narrow overlap of the polymer absorption band with the solar spectrum; (2) inefficient exciton splitting due to poor donor and acceptor interfacial interactions; (3) low charge carrier mobility; and (4) low efficiency of charge transport across the interface with the electrode.

Different approaches are being pursued based on optimizing different steps involved in the OPV operation in an attempt to increase the PCE. One such approach is the fabrication of lower bandgap polymers[9–15] that can absorb a wider energy range of solar photons than P3HT and hence harvest photons more effectively. Typically, two synthetic approaches are used in lower bandgap polymers: (1) designing copolymers of alternating push−pull donor and acceptor blocks, which lowers the polymer bandgap by creating a quasi charge transfer state in the polymer backbone[16,17] and (2) adding fused rings to monomer blocks, which stabilize the quinoidal character of a conjugated backbone.[18,19] In many low bandgap polymers, both the donor−acceptor and quinoidal characteristics are present. The effects of the aforementioned mechanisms have been previously studied for several heterocyclic polymer and oligomer materials.[20–24]

It is also worth mentioning that lowering the bandgap in electron donor polymer materials has to balance with having sufficient driving force for exciton splitting and the optimal open circuit voltage in OPV devices. On one hand, lowering the bandgap will increase the efficiency for exciton generation; on the other hand, it also sometimes lowers the driving force for exciton splitting and decreases the open circuit voltage. As an example, polythieno[3,4-*b*] thiophene has a bandgap as low as 0.85 eV,[25,26] but it has neither a high exciton splitting efficiency nor an ideal open circuit voltage for photovoltaic devices because of insufficient driving force for exciton splitting using typical electron acceptors, such as PCBM. Therefore, for solar cell applications, thienothiophene units need to be connected to another kind of conjugated monomer, such as thiophene or benzodithiophene, to tune the bandgap for optimized PV performance. Using this technique, efficiencies of almost 8% have been realized.[27–30] This diblock copolymer approach has been demonstrated by our previous studies on a series of random copolymers with thiophene(T)/thienothiophene(TT) ratios of 1,

† Part of the "Michael R. Wasielewski Festschrift".

* Corresponding authors. E-mail: lchen@anl.gov, lupingyu@uchicago.edu.
‡ Department of Chemistry, Northwestern University.
§ Argonne National Laboratory.
∥ Argonne-Northwestern Solar Energy Research (ANSER) Center, Northwestern University.
⊥ The University of Chicago.

10.1021/jp101925b © 2010 American Chemical Society
Published on Web 05/21/2010

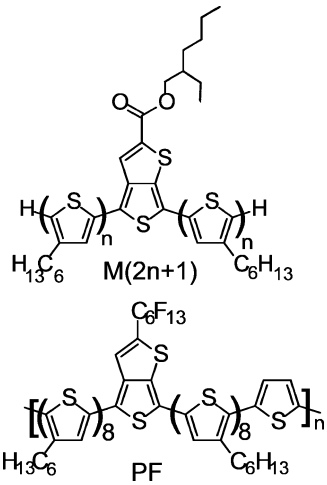

Figure 1. Chemical structures of the oligomers M(2*n*+1) (where $n = 0$, 1, 2, 4, and 8) and polymer PF.

3, 5, 9, and 14, in which we reported their energy gaps, absorption spectra, and bulk heterojunction (BHJ) OPV device (with PCBM) efficiencies.[31] The studies have shown that the OPV cells have the highest solar cell efficiency when the T/TT ratio is an average of 9 in a random sequence, which was named Copolymer C. However, compared with the others in the series, Copolymer C does not have the broadest absorption in the solar spectrum. This observation suggests that other fundamental factors related to the low bandgap copolymer motif contribute to the PCE of the material in BHJs. A regioregular polymer has also been fabricated as a means to more accurately determine the interactions between the thienothiophene and thiophene units.[32] To understand fully how to optimize OPV device performance, we need to understand the fundamental steps in the OPV functions of these polymers at a molecular level. It is important to understand the unique characteristics of conjugated copolymers within the context of their OPV functions and their difference with homopolymers beyond merely harvesting more solar photons. The results will be compared with the better-known oligothiophene (OTH) or thiophene units with other fused systems.[1,10]

In our studies reported here, four co-oligomers have been synthesized, each of which consists of one thieno[3,4-*b*] thiophene derivative (denoted TT) unit at its center linked at both ends with one alkyl OTH fragment (Figure 1).[31–33] The OTH fragments are one, two, four, or eight thiophene units in length. The co-oligomers are hence named M3, M5, M9, and M17, with their numbers corresponding to the total monomer units in the co-oligomers. The structure of these oligomers is shown in Figure 1. A fluorinated, polymerized form of the M17 molecule, PF, is also shown. Although the main emphasis of this article is on the length dependence of the oligomer series, the transient optical anisotropy of the PF polymer compared with P3HT will also be discussed as a means to discuss the exciton diffusion aspects in the polymer series. We hope to use these models to gain further insight into the nature of charge and electron flow between OTH and TT units in the low-bandgap copolymers. Specifically, we would like to characterize both electronic and intrachain structural effects arising from the addition of the fused ring in the TT unit to these co-oligomers. This study will compare the initial electronic states and electron transport mechanisms of these molecules with the more conventionally used OTH species, which have been studied extensively in the past.[2,34–40] In this report, the above-mentioned interactions characterized by the experimental absorption, fluorescence, and time-resolved fluorescence spectra are discussed and compared with a theoretical assessment of the studied structures. In this study, we hope to shed some light on three basic questions that are of current interest in conjugated materials: (1) What is the effect of the TT fused ring on a conjugated backbone system and how long spatially can a single fused ring affect the backbone? (2) What are the electronic and structural implications for the electron localization and exciton diffusion for these materials? (3) Can these effects be related to polymers properties and functions observed experimentally, such as current density and solar cell efficiency?

2. Experimental Section

Four model oligomers, M3, M5, M9 and M17, are studied, and their structures are shown in Figure 1. The synthesis of these molecules is described in the Supporting Information. The synthesis of PF was previously reported.[32] The molecular concentrations in toluene or chlorobenzene were 10^{-4} to 10^{-5} M. Within this concentration range, the absorption and fluorescence spectra do not change in shape, indicating that effects of aggregation are minimal. The absorption and fluorescence spectra were obtained using a Shimadzu UV-2401PC recording spectrophotometer or a Shimadzu UV-1609 spectrophotometer and by a PTI fluorescence master series fluorimeter or a Shimadzu RF-5301PC spectrofluorophotometer, respectively.

For the fluorescence upconversion measurements, a 100−250 kHz Coherent RegA system centered at 790 nm was used. Part of the light was directed into an optical parametric amplifier (OPA) to create ultrafast pulses in the visible range (490−720 nm), whereas another portion of the light was used as the 790 nm gate pulse. Both the visible and 790 nm beams were directed into an Ultrafast Systems Halcyone fluorescence setup. The 790 nm beam was directed to a retroreflector attached to a variable translation stage. The visible light was focused into a 2 mm path length cuvette containing the solutions studied. The solutions were stirred using a small magnetic stirrer to minimize effects such as heating and sample degradation. The solution samples were studied within a few hours of when they were dissolved. The fluorescence signals passed through a long-pass filter. The fluorescence light and the 790 nm light were then focused onto a BBO crystal cut to optimize the sum frequency generation (SFG) of the signal. The SFG signals were created when the fluorescence and gate pulses were combined in the crystal and were directed into a monochromator and single-photon-counting PMT setup. The instrument response function was <400 fs. We obtained the kinetics trace by varying the time delay between the excitation pulse and the gate pulse through moving the variable translation stage connected to the gate pulse. The detection wavelengths were changed using the monochromator. Because the efficiency of the SFG changes as a function of the wavelength and crystal angle, the crystal angle is optimized for each kinetics trace at the different wavelengths.

The electronic structure and energy calculations were performed using Hyperchem (Hypercube). The geometries were optimized using the AM1 semiempirical method, whereas the energetic and spectroscopic characteristics were calculated using the ZINDO/S package included in Hyperchem.

3. Results

3.1. Experimental Results. The steady-state absorption and fluorescence spectra are shown in Figure 2 for the M3, M5, M9, and M17 molecules in toluene solutions. Two main peaks observed in the absorption spectra are tentatively assigned to

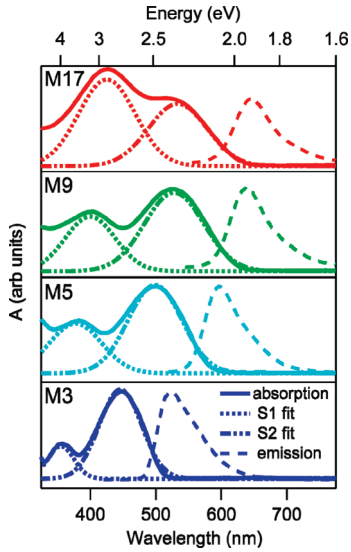

Figure 2. Absorption (solid line) and emission spectra (dashed line) of the M3−M17 oligomers. The spectra are offset for clarity. The individual fits of the S1 and S2 peaks in the absorption spectra are also indicated (dotted and dashed-dotted lines).

TABLE 1: Numerical Results for the Absorption and Emission Spectra Shown in Figure 2

	S1 nm (eV)	S2 nm (eV)	emission nm (eV)	Stokes shift (eV)
M3	446 (2.78)	355 (3.49)	524 (2.37)	0.41
M5	498 (2.49)	377 (3.29)	597 (2.08)	0.41
M9	528 (2.35)	397 (3.12)	637 (1.95)	0.40
M17	535 (2.32)	425 (2.91)	643 (1.93)	0.39

S1 and S2, corresponding to the $S_1 \leftarrow S_0$ and $S_2 \leftarrow S_0$ transitions, respectively. The absorption peaks were fit to individual Gaussian functions, as shown in Figure 2 and Table 1. A progressing red shift of both peaks is observed as the molecular length increases. This suggests that the electron delocalization length in the excited state increases with the oligomer size. Although there is a slight bathochromic shift of the S1 peak for M17 when compared with M9, an obvious saturation of the shift as a function of the length is observed for this molecule. The S1 peak for the longest oligomer M17 is at 2.31 eV (535 nm), which is much lower in energy compared with the lowest energy peak in the absorption spectrum of P3HT in solution at 2.76 eV (450 nm).[41,42] In comparison with poly thieno[3,4-*b*]thiophene, or poly-TT, the peak maximum of the unsubstituted polymer was found to be 1.62 eV (764 nm) in water,[43] and the oxidized film bandgap can be as low as 0.85 eV (1460 nm).[26] In addition, poly-(T-TT), which was reported in one of our previous studies, has an absorption peak at ~1.65 eV (750 nm) and a shoulder at 1.46 eV (850 nm) in chlorobenzene.

The fluorescence spectra of the M series oligomers are also shown in Figure 2. The peak maxima are shown in Table 1. The peak maxima follow the same trend as the lower energy peaks in the absorption spectra. The large Stokes shift and vibrational broadening most likely have contributions from conformational changes between the excited and ground states. The molecules relax from a puckered to a more planar configuration in the excited state, which will be discussed in more detail in the next section. For the M9 molecule, the peak width (fwhm) of S1 is 0.28 eV, whereas the peak width of the fluorescence is 0.19 eV. In contrast, the OTHs with the same backbone length have an absorption bandwidth of 0.7 eV and

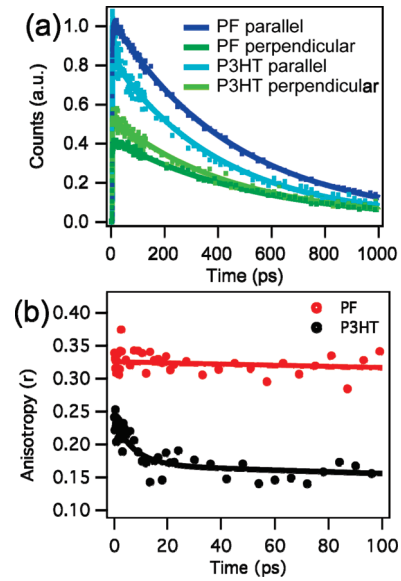

Figure 3. (a) Polarization-dependent fluorescence lifetimes for PF and P3HT obtained using fluorescence upconversion. The excitation wavelength for PF was 550 nm, whereas the excitation wavelength for P3HT was 500 nm because the optical bandgap for P3HT is higher. The emission wavelength detected was 700 nm for PF and 630 nm for P3HT. The changes in the relative vertical and horizontally polarized excitation pulses reflect the molecular orientation in the medium. (b) Measured temporal anisotropy (dots) and anisotropy fits (straight lines) for the PF (red) and P3HT (black) polymers. We obtained the anisotropy by using the data from Figure 3a and using the relationship in eq 1.

a fluorescence bandwidth of 0.4 eV in solution.[44,45] The Stokes shift for the M3 molecule is 3337 cm^{-1}, whereas the Stokes shift for the M17 molecule is 3139 cm^{-1}. Although this is a relatively large spectral shift, it is smaller than the Stokes shift typically observed for alkyl substitutes OTHs, which have Stokes shifts as high as 0.87 eV (7017 cm^{-1}).[46] The Stokes shift has various origins, such as the vibrational relaxation of the excited state and conformational changes. The smaller Stokes shift relative to the OTHs suggests that the structural changes in the excited state relative to the ground state are smaller, which coincides with the calculations discussed below and in the Supporting Information. Another interesting point is that the fluorescence spectra do not show vibronic characters at room temperature. This is also in contrast with the alpha OTHs,[47] where the quinoidal character of the excited state stiffens the backbone chain, which accounts for both the enhancement of the vibronic peaks and the spectral narrowing in the fluorescence spectra.[34] The broadening of the fluorescence bands in the T/TT oligomers studied here indicates that either the structure of the excited state is not as rigid as in the homocyclic OTHs or the ground state already has a more rigid backbone than P3HT. This topic will be discussed in more detail in the Discussion.

To investigate the rigidity of PF in comparison with P3HT, we carried out fluorescence anisotropy measurements using the fluorescence upconversion.[48] The polarization-dependent signals of time-resolved fluorescence for the PF and P3HT polymers in chlorobenzene are shown in Figure 3. The excitation wavelength for the PF polymer was 550 nm, whereas the detection wavelength was set to 700 nm. For the P3HT polymer, the excitation wavelength was 500 nm and the fluorescence wavelength was set to 630 nm. These wavelengths were chosen to negate higher energy relaxation contributions. The polarization of the pump was varied, whereas the polarization of the 790 nm gate was kept constant. By changing the relative

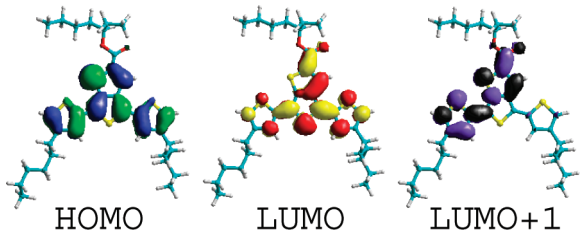

Figure 4. HOMO (left, green and blue), LUMO (middle, red and yellow), and LUMO+1 (right, violet and black) orbitals in M3.

polarization of the pump and gate pulse trains, the amplitude and dynamics of the molecular orientation are mapped out simultaneously. The time-dependent anisotropy of the signals can be measured by the relationship

$$r(t) = \frac{I_{\parallel}(t) - I_{\perp}(t)}{I_{\parallel}(t) + 2I_{\perp}(t)} \quad (1)$$

where r is the anisotropy, $I_{\parallel}$ is the signal intensity at the delay time, t, where the gate and excitation pulses have the same polarization, and $I_{\perp}$ is the intensity at time t where the gate and excitation pulses are orthogonally polarized. We determined the isotropic decay of the fluorescence by measuring the fluorescence upconversion with the pump and probe beams at the magic angle (54.7°). A 500 ps decay was determined for the PF polymer, and a 450 ps decay was measured for the P3HT polymer in chlorobenzene. For the PF polymer, the measured anisotropy decay is several nanoseconds. Because the fluorescence decay of the signal is 500 ps, the anisotropy cannot be accurately measured for this system. What can be determined is that (a) the anisotropy decay can be approximately expressed using one time constant and (b) there is no indication of a fast anisotropy decay component within the instrument response range (300 fs) of this system. The initial anisotropy for PF is $r(0) = 0.32$. The fluorescence anisotropy of the P3HT molecule has also been previously measured as well as measured in this study as a reference,[48] where the decay kinetics could not be expressed by a simple exponential function. Instead, the P3HT fluorescence anisotropy decay kinetics was previously expressed by up to four exponential components with time constants ranging from 1 to 300 ps. The absence of the fast anisotropy decay component in PF suggests nonexistence of internal rotation and intrachain exciton migration associated with the dihedral angles between adjacent units due to its higher backbone rigidity compared with P3HT. The longer decay components in both polymers show a similar trend.

3.2. Calculations. To elucidate further the nature of the ground and excited states for the M series oligomers, semiempirical quantum mechanical calculations were performed using Hyperchem (Hypercube, Inc.) software. As a reference, structures and energies of the corresponding thiophene oligomers were also calculated and compared with these previously reported results.[36] The frontier molecular orbitals of the HOMO, LUMO, and LUMO+1 for M3 are shown in Figure 4. By analyzing the ZINDO/S calculations, the first allowed $S_1 \leftarrow S_0$ transition has ~100% HOMO → LUMO character, which indicates that the electron density shift between the S_1 state and the S_0 states can be adequately expressed by the electron density shift from HOMO to LUMO. This transition corresponding to the S1 peak has an energy value of 2.67 eV (464 nm), which is in good agreement with the experimental value of 2.78 eV. The nature of the HOMO and LUMO levels for M3 closely resembles that of the unsubstituted OTHs. The LUMO is also similar to that of the terthiophene molecule, but the electron density is higher at the TT moiety. The electron density shifts toward the center of the molecule. For M3, the HOMO and the LUMO show full delocalization. For LUMO +1, however, TT breaks the conjugation of the polymer backbone. The orbital diagram shows that most of the electron density is situated around half of the molecule and the TT unit.

The frontier molecular orbitals for M5, M9, and M17 are shown in Figure 5. Because the alkyl side groups are not electronically active and do not significantly affect these orbitals, they were substituted with methyl groups for simplicity. The red shift of the two lowest transitions as a function of chain length is mimicked in these calculations. The LUMOs and HOMOs for M5 extend over the entire conjugated backbone. However, the LUMO for M17 only spans through seven to eight monomer units or ~2.5 nm in length, whereas the HOMO extends through the entire oligomer backbone of 7.1 nm in length. In contrast, the LUMO for a 17-mer oligo-T spans through the entire backbone. The HOMO → LUMO transitions for the diblock oligomers draw the electron density from the entire backbone toward the central TT unit, which is the origin of the charge transfer character in the M series to be discussed later. The electron density shift due to the HOMO → LUMO transition is more apparent in the longer diblock oligomers. The exciton delocalization range for M17 is significantly smaller compared with P3HT, which is typically measured to be 3−8.5 nm.[49–51] Although the exciton diffusion length is typically longer than the conjugation length because of exciton hopping mechanisms that will be discussed in the Discussion, longer conjugation lengths can enhance the exciton diffusion length as well as lower the bandgap of the material.

The calculated HOMO and LUMO energy levels as a function of the inverse of the chain length in terms of the number of monomer units, n, for the thiophene (T), thienothiophene (TT), and M series oligomers are shown in Figure 6. For the TT oligomers, a COOH group was added to the TT unit for these calculations, and the resulting effects on the HOMO and LUMO energy levels will be discussed later in this section. Because the $S_1 \leftarrow S_0$ transition is almost 100% HOMO−LUMO in character, these MO energy levels should mainly affect the position of the lowest energy peak in the electronic absorption spectrum. M3 shows less than a 0.1 eV shift relative to the HOMO level of T3, but the LUMO shifts by over 0.2 eV. The HOMO levels do not vary greatly between T and M series oligomers investigated. In contrast, the LUMO for the M series is significantly lower compared with the T oligomers. The HOMO and LUMO energy gaps for the TT oligomers are much lower. When studying the LUMO levels more carefully, it is observed that the homo-oligomers (T and TT) show a good linear dependence for both the HOMO and LUMO energy levels versus the inverse number of rings in the backbone. For the M series, the HOMO level shows a linear dependence, whereas the decrease in the LUMO level saturates at roughly eight thiophene units. Therefore, it was observed that the experimental data, molecular orbital pictures, and HOMO and LUMO levels all indicate an initial saturation of the first excited state at seven to eight units.

Although it has been established that the first excited state is partially localized in the M series from the MO and energy level calculations, this phenomenon does not fully explain the reduced bandgap of this transition. The lower transition energy is typically attributed to either (a) an increase in the quinoidal

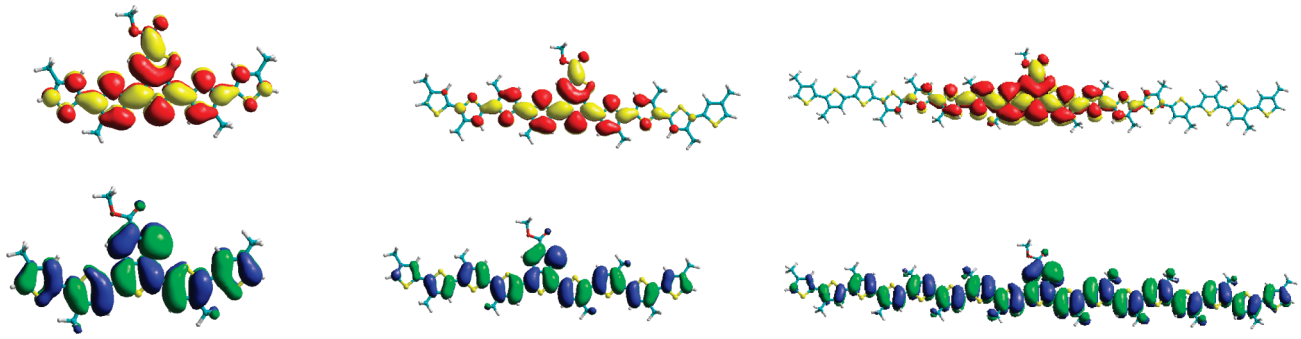

Figure 5. Frontier orbitals (LUMO, top; HOMO, bottom) of the M5 (left), M9 (middle), and M17 (right) oligomers. As the molecular size increases, the conjugation in the LUMO orbital is suppressed.

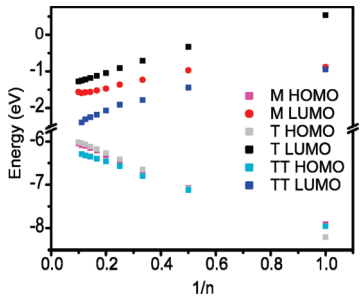

Figure 6. Chain length dependence of HOMO and LUMO energy levels versus the inverse chain length for the M series (M), thiophene (T), and thienothiophene (TT) oligomers.

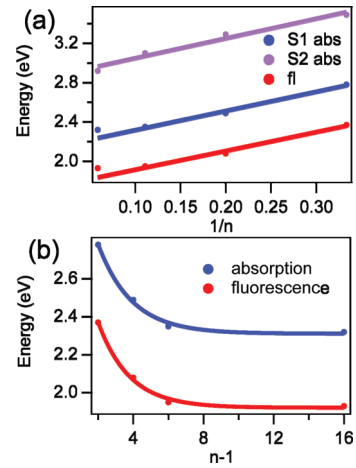

Figure 7. (a) Energy position of the absorption and emission spectra indicated in Figure 2 as a function of the inverse chain length. (b) Experimentally obtained dependence of the S1 absorption peak and fluorescence peak as a function of chain length. The latter relationship is used to better characterize the effective conjugation length of the M series oligomers.

character of the ground state versus the typically aromatic character of higher bandgap materials or (b) the donor−acceptor nature of diblock polymers in the backbone chain. The aromatic form of the molecule has more electron density inside the thiophene rings, whereas the quinoidal character has an enhanced electron density in the bonds between the thiophene rings, which in turn shortens these bonds. A thorough investigation of the ground- and excited-state geometry was performed on the M series oligomers and is shown in the Supporting Information. The TT-T sequential arrangement along the backbone chain also creates a donor−acceptor mechanism in these oligomers. The details of the calculated geometric structure, along with the bond alternation and aromaticity of these structures, are shown in the Supporting Information. These calculations indicate that the lower bandgap in the M series is mainly due to the donor−acceptor nature between the TT and T units. This lower energy transition is ascribed to a partial donor−acceptor charge transfer state where the TT ring acts as a partial electron acceptor and the end thiophene rings act as partial electron donors. This will be discussed in more detail in the Discussion.

4. Discussion

4.1. Conjugation Length Dependence of the S_1 State. From the calculations, and the absorption and emission spectra, we have observed that the main difference in these oligomers is that the TT unit lowers the energy of the $S_1 \leftarrow S_0$ transition. Although this result was expected, it is not clear to what extent spatially a single fused TT ring can influence energy levels of the overall OTH backbone. The relationship of the S1 absorption peak energy and the fluorescence peak energy versus $1/n$ (where n is the number monomer units in the oligomer backbones) are shown in Figure 7a. This dependence is linear for M3, M5, and M9, but seems to reach a plateau for M17, which has a higher energy than the projected linear dependence, showing a saturation of the conjugation length. In contrast, the S2 peak energy versus $1/n$ shows a roughly linear dependence for the entire series, which is also shown in Figure 7a. The trends observed in Figures 2 and 7a both indicate that (a) the TT unit substantially lowers the bandgap of the oligomers and (b) the effect of TT on the S1 peak from the $S_1 \leftarrow S_0$ transition is more localized than that on the S2 peak from $S_2 \leftarrow S_0$ transition. The question is therefore what the natures of the two transitions are, as discussed below.

To more accurately determine the conjugation length of the S_1 state, the relationship between the optical bandgap and the oligomer backbone units was determined. It is well known that for longer oligomers, the optical bandgap of the material can become saturated, which then follows the relationship[52]

$$E(n) = E_\infty + (E_1 - E_\infty)\exp[-s(n-1)] \qquad (2)$$

where E_∞ is the limiting optical bandgap for $n \rightarrow \infty$, E_1 is the energy of the monomer, s is a parameter related to the saturation length of the molecule, and n is the number of monomer units. The S1 absorption and fluorescence peaks both fit this relationship (Figure 7b). For the M series absorption spectra, $E_\infty = 2.31$ eV ($\lambda = 537$ nm), whereas for their fluorescence spectra, $E_\infty = 1.92$ eV ($\lambda = 646$ nm). The average s parameter of M series from the absorption and fluorescence fits was 0.54 ± 0.02. With

this parameter, the bandgap of the M series oligomers reaches over 95% saturation within seven monomer units. If the effective conjugation length is defined as the smallest number of units in which the optical bandgap differs by <1 nm compared with the limiting optical bandgap (in nanometers), then the effective conjugation length for the S_1 state is 11 units. In comparison, the bandgap of P3HT in solution is 2.76 eV ($\lambda = 450$ nm),[41,42] and the effective conjugation length for oligo-T is 17−20 units.[52] Therefore, the S1 peak in the M series oligomer is clearly red-shifted because of the presence of the middle TT unit, and the effective conjugation length for the M series oligomers is roughly one-half of that for their oligo-T counterparts. The peak maximum of the unsubstituted poly-TT was found to be 1.62 eV ($\lambda = 764$ nm) in water[43] and 0.85 eV ($\lambda = 1460$ nm) in oxidized films.[26] A copolymer made of alternating T and TT units, which has been previously reported, has a maximum absorption at roughly 1.65 eV ($\lambda = 750$ nm) and a shoulder at 1.46 eV ($\lambda = 850$ nm) in chlorobenzene.[31,53] The TT oligomers have not been studied to date, so the effective conjugation length is unknown. Nevertheless, we have shown that (a) the optical bandgap of the conjugated oligomer species can be tuned by varying the ratio of higher bandgap and lower bandgap moieties and (b) the effective conjugation length of the S_1 state is surprisingly long considering that the electronic state is formed by the effects of a single lower bandgap unit.

The S_1 state in M series oligomers does show a delocalization for three to four thiophene units on each side of the middle TT unit. The red shift of the lowest energy transition energy as a function of the backbone length is interpreted to be a charge-localized perturbation of the thiophene ground state. It is interesting to note that the saturation parameter, s, in eq 2 is 0.54, which is smaller than that of structurally similar oligomers with lower bandgaps, which have $s = 0.85$.[21] On the other hand, oligo-T derivatives with higher bandgaps have $s = 0.4$,[52] which further indicates that they have longer conjugation lengths compared with the M series oligomers. The M series oligomers have an intermediate exciton diffusion length in the comparisons mentioned above. Therefore, these oligomers could have an optimal relationship between the conjugation length and the bandgap energy value. The lower bandgap diblock oligomers have shorter conjugation lengths and more localized strongly interacting species. Consequently, the shorter conjugation lengths in diblock oligomers compared with homo-oligomers can have a negative effect on exciton diffusion because the energy gradient due to the charge transfer nature around each lower bandgap unit will effectively act as an exciton "trap" to slow down its diffusion along the backbone. The intrachain exciton diffusion length along the polymer backbone is therefore longer for homopolymers compared with diblock copolymers with more locally charged species. Therefore, the donor/acceptor domain spatial separations in the polymer/PCBM films for the BHJ solar cell need to be smaller for those materials based on multiblock copolymers than those of homopolymers. Devices with smaller domain sizes with lower bandgaps will be a recommended combination for enhancing solar cell performance. This will be discussed in more detail below.

The energy of the S2 peak versus the length of the oligomer was also investigated in more detail. The effective conjugation length for the S_2 state is longer compared with the S_1 state. By having different electronic states with varying conjugation lengths, it is possible to further control the exciton diffusion within the conjugated backbone chain. The S2 peak energy in the co-oligomer species is similar to that of the lowest energy transition peak in OTHs with roughly only one-half of the size.

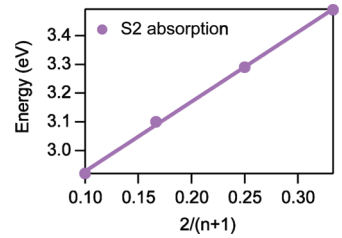

Figure 8. Energy level of the S2 peak as a function of the inverse chain length. This relationship indicates that the conjugation in this state covers only half of the molecule

For instance, the S2 peak for M9 ($n = 9$) is at 397 nm, whereas penta-thiophene ($n = 5$) absorption maximum is at 398 nm.[54] In comparison, thiophene nonomer ($n = 9$) has a peak maximum at 437 nm. Therefore, it is assumed that the transition state presented by the S2 peak contains $(n + 1)/2$ units, where n is the number of the monomer units in the backbone. Because the S2 peak is tentatively assigned to the $\pi-\pi^*$ transition along the thiophene backbone, the above relationship suggests that the conjugation associated with this particular transition is delocalized over half of the oligomer and ends with the thienothiophene unit. The relationship between the S2 peak energy and $2/(n + 1)$ is shown in Figure 8. This is also in good agreement with the calculated molecular orbitals. This relationship follows a more linear behavior compared with the $1/n$ relationship shown for this state in Figure 7a and also fits well to the unsubstituted thiophene spectra. Because no saturation of the excited state was observed in these experiments, a more simplistic linear relationship is assumed rather than the relationship described in eq 2. Although the conjugation only spans half of the molecule, the S_2 state has a higher electron density on the edge of the molecule. Therefore, exciton localization to the center of the molecule can be enhanced for molecules that are excited to the S_2 state.

4.2. Charge Transfer Contributions to the Fused Ring Bandgap Reduction. For low bandgap oligomers and polymers consisting of diblock sequences with combinations of thiophene and another lower bandgap fused-ring unit, there are typically two main components responsible for the red shift of the bandgap onset: the admixing of quinoidal character in the ground state due to the fused thiophene rings on the thiophene backbone and the charge transfer character resulting from different electron affinities of the neighboring units.[10] The absorption and fluorescence spectra can indicate the quinoidal or charge transfer character of the material investigated, but theoretical analysis is needed to characterize fully the nature of the bandgap optimization in the M series. The experimental and calculated results show that the lower energy transition does not completely change the aromatic character of the ground state, but the central component of the oligomers is slightly higher in quinoidal character. This electronic character slightly stiffens the molecules, so the structural differences between the ground and the excited state are minimized.

The relative stabilities measured by the calculated formation energy of several aromatic and quinoidal homopolymers and oligomers have been previously studied.[40] In the theoretical calculations previously described, the aromatic structure of the TT polymer was predicted to be lower than its quinoidal structure by 0.3 kcal/mol, whereas that of the TT dimer was more stable by 11.1 kcal/mol.[40] Apparently, this energy difference increased as the oligomer size decreased. Therefore, it was discovered that the relative quinoidal component for the TT

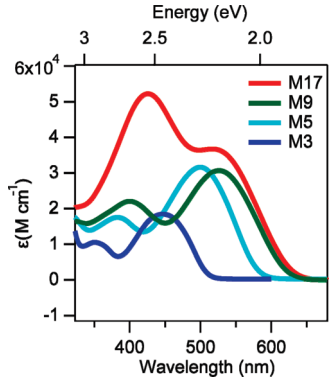

Figure 9. Wavelength-dependent extinction coefficients of the M series oligomers. The extinction coefficient of the S2 peak increases linearly with the chain length, whereas the S1 peak does not increase considerably for oligomers longer than M9.

oligomer is higher than that of the T oligomer. Therefore, the bandgap of the poly-TT is lower than that of poly-T but higher than poly(isothianaphthene) with more quinoidal character and an even lower bandgap. The quinoidal character for the M series oligomers is also reduced compared with the corresponding oligomers with a quinoidal thiophene units. For instance, it has recently been reported that a bithiophene derivative with a highly quinoidal structure has an absorption maximum at ~550 nm.[55] This is lower in energy than the S1 peak in the M3 oligomer. Therefore, we can assume that the ground state is mainly aromatic in nature for all of the oligomers. The lower bandgap stems from a donor−acceptor charge transfer character of the neighboring T and TT units. Although this discrepancy is centered around the TT unit in the ground state, the excited state shows a more significant change in the bond distances compared with comparable OTH segments.

4.3. Absorption Ratios and Exciton Diffusion. The spectral extinction coefficients of each monomer studied are shown in Figure 9. When comparing the ratios of the S1 and S2 peak extinction coefficients of each molecule, the extinction coefficients of the S1 peak in M5−M17 are similar. In contrast, the extinction coefficient for the S2 peak is much greater for M17. The oscillator strength is related to the extinction coefficient by the relationship $f \approx 4.31 \times 10^{-9} \int \varepsilon(\nu)\, \mathrm{d}(\nu)$[56] where f is the oscillator strength, ε is the extinction coefficient, and ν is the spectral frequency. Because the spectral widths of the peaks shown in Figure 9 do not vary significantly, a direct relationship between f and ε is assumed. The increase in ε as a function of the backbone length is characteristic of a fully conjugated system. Typically, f scales linearly with the number of rings in the backbone that are within the conjugation length.[57] The relative change in the intensities of these two peaks further indicates that the lower energy peak has contributions from a localized state due to the TT unit whereas the higher energy peak is from the oligo-T segments in the backbone. The ratio of these peaks can also have implications on the light harvesting from the sun. Increasing the spectral overlap with the solar spectrum is one of the main benefits of using low bandgap polymers. The utilization of both the lower energy absorption by the localized charge-transfer-originated transition and the higher energy absorption by the delocalized transitions can increase the overall light harvesting efficiency of the polymer. Using this rationale, the M9 co-oligomer should show the best light harvesting property compared with other oligomers in the M series for the following reasons: (1) the absorption band energy is lowered to capture more photons and (2) the extinction coefficient for the lowest energy S1 peak compared with that of larger oligomers does not decrease significantly. For the M17 molecule, the bandgap does not significantly decrease for increased overlap with the solar spectrum, and the S1 peak extinction coefficient is essentially the same as that of M9. Meanwhile, M17 is larger than M9, so there are fewer absorbers in films with the same unit mass and unit thickness of the material. From previous studies on photovoltaic performances of poly-T-TT copolymers with random sequences but well-defined stoichiometry ratios of T/TT, it was determined that the copolymer C most closely resembling the M9 oligomer sequence gave the highest PCE in devices.[31] This further validates the above analysis. Compared with the M series co-oligomers, the copolymers with random sequences showed a single broad peak instead of two distinctive peaks due to statistically diverse sequences resulting in diverse energies in the S1 and S2 peaks.

The fluorescence anisotropy of a conjugated polymer, such as PF or P3HT, measures the dynamics for the exciton dipole randomization due to exciton hopping or diffusion via intrachain and interchain mechanisms. It is also a way to investigate the polymer morphology in films or conformation in solution. Torsional motions along the polymer backbone will shorten the conjugation length in P3HT, which is ~20 monomers in a planar backbone conformation. The initial excitation of the polymer is concentrated on a short segment of the entire backbone, followed by the exciton migration through the backbone via a Förster type hopping mechanism.[58] In solution, intrachain exciton hopping dominates. If the polymer has a randomly coiled conformation facilitated by torsional motions along the backbone, then the exciton dipole orientation will become randomized as a result of this hopping mechanism. The fast fluorescence anisotropy decays observed in P3HT are attributed to this hopping mechanism. In the PF polymer, however, this rapid exciton dipole randomization due to the exciton hopping is not observed. Therefore, we can deduce that the hopping mechanism is not significant in PF. Because the polymer consists of a localized state similar to the oligomer species, the exciton cannot migrate to other S_1 states in the system. In other words, the TT units effectively set traps for the excitons and prohibited their migration along the backbone. The much longer anisotropy decay of over 1 ns is due to the overall polymer molecule rotational diffusion. This exciton confinement hence requires a nearby electron acceptor to split the exciton into charges and a much higher miscibility between the donor polymer and acceptor, such as PCBM to have high PCE. It has been previously shown that the PF has a lower charge mobility compared with P3HT. The confinement of the exciton to a single fragment centered around a TT unit is likely contributing to this effect, even though the exciton diffusion and charge diffusion mobilities are not the same. The excitons can still travel to neighboring polymer strands through π-stacked chains. This finding has implications on the interplay between the exciton diffusion and spectral overlap of the materials. By lowering the bandgap of the material, exciton migration can also be hindered along the polymer backbone. Although the mobility of the PF material is lower compared with P3HT, the current density, which is one of the main indicators of solar cell efficiency, is over 10.2 mA/cm.[2] This parameter is higher than that reported for P3HT solar cells with >5% efficiency.[59] The molecular weight of PCBM is 910.9 g/mol, and the diameter of PCBM is ~1 nm. These parameters are nearly the same as those of M5. Typically, polymer/oligomer blends with PCBM are optimized at roughly a 1:1 weight ratio.[28,30,32,59] If the exciton diffusion

length is comparable to the mean distance between PCBM acceptor molecules at the polymer/PCBM interface, then the migration effect can be minimal. This dependence will be probed further in future works.

5. Summary

We have studied a well-defined thiophene-thieno[3,4-*b*]thiophene oligomer series to determine the electronic and structural effects on a single fused thienothiophene in a thiophene backbone chain of varying length. The ground-state electronic spectra show characteristics similar to the OTH states reported previously, but a low-energy first excited state peak is observed. The fused thienothiophene ring does not significantly alter the ground state, but the excited state shows an enhanced aromatic character compared with OTHs, which minimizes the structural difference between the ground and excited states. The effect of the thienothiophene ring appears to extend to roughly seven to eight monomer units. The first excited state is lower by 0.37 eV for the polymer or longer oligomer homocyclic thiophene species. The electron density of this state is concentrated in the center of the molecule, which indicates that a partial charge transfer is responsible for this state. The second excited state closely resembles the first excited state of an unsubstituted OTH with roughly half as many thiophene rings. Therefore, it is assumed that the fused ring breaks the conjugation for this state, but it is delocalized for half of the molecule. The conjugation for the M3−M9 units shows a linear dependence of the energy shift versus 1/*n*. The saturation of this peak appears to occur at seven to nine units. This conjugation saturation has consequences for intrachain charge transfer and exciton diffusion. The overall spectral characteristics of these materials lead to an enhanced current in photovoltaic devices.

Acknowledgment. This work is supported by the Division of Chemical Sciences, Office of Basic Energy Sciences, the U.S. Department of Energy under contract DE-AC02-06CH11357 (for L.X.C.). We gratefully acknowledge the financial support of the National Science Foundation and the NSF MRSEC program at the University of Chicago. The UC/ANL collaborative seed grant (L.Y. and L.X.C.) and the Setup fund from Northwestern University (L.X.C.) provided partial support of this research. The most recent fluorescence upconversion anisotropy work was supported as part of the ANSER Center, an Energy Frontier Research Center funded by the U.S. Department of Energy, Office of Science, Office of Basic Energy Sciences, under award number DE-SC0001059. We would also like to thank Carmen Herrmann for helpful discussions.

Supporting Information Available: Molecular synthesis, NMR characterization, detailed theoretical geometric analysis, and theoretical TT substituent effects. This material is available free of charge via the Internet at http://pubs.acs.org.

References and Notes

(1) Dennler, G.; Scharber, M. C.; Brabec, C. J. *Adv. Mater.* **2009**, *21*, 1323.
(2) Yu, G.; Gao, J.; Hummelen, J. C.; Wudl, F.; Heeger, A. J. *Science.* **1995**, *270*, 1789.
(3) Brabec, C. J.; Sariciftci, N. S.; Hummelen, J. C. *Adv. Funct. Mater.* **2001**, *11*, 15.
(4) Gunes, S.; Neugebauer, H.; Sariciftci, N. S. *Chem. Rev.* **2007**, *107*, 1324.
(5) Padinger, F.; Rittberger, R. S.; Sariciftci, N. S. *Adv. Funct. Mater.* **2003**, *13*, 85.
(6) Reyes-Reyes, M.; Kim, K.; Carroll, D. L. *Appl. Phys. Lett.* **2005**, *87*, 083506.
(7) Scharber, M.; Mühlbacher, D.; Koppe, M.; Denk, P.; Waldauf, C.; Heeger, A.; Brabec, C. *Adv. Mater.* **2006**, *18*, 789.
(8) Sirringhaus, H.; Brown, P. J.; Friend, R. H.; Nielsen, M. M.; Bechgaard, K.; Langeveld-Voss, B. M. W.; Spiering, A. J. H.; Janssen, R. A. J.; Meijer, E. W.; Herwig, P.; de Leeuw, D. M. *Nature.* **1999**, *401*, 685.
(9) Bredas, J. L.; Heeger, A. J.; Wudl, F. *J. Chem. Phys.* **1986**, *85*, 4673.
(10) Bundgaard, E.; Krebs, F. *Sol. Energy Mater. Sol. Cells* **2007**, *91*, 954.
(11) Cheng, K.; Liu, C.; Chen, W. *J. Polym. Sci., Part A: Polym. Chem.* **2007**, *45*, 5872.
(12) Morana, M.; Wegscheider, M.; Bonanni, A.; Kopidakis, N.; Shaheen, S.; Scharber, M.; Zhu, Z.; Waller, D.; Gaudiana, R.; Brabec, C. *Adv. Funct. Mater.* **2008**, *18*, 1757.
(13) Mühlbacher, D.; Scharber, M.; Morana, M.; Zhu, Z.; Waller, D.; Gaudiana, R.; Brabec, C. *Adv. Mater.* **2006**, *18*, 2884.
(14) Tamura, H.; Yamanaka, S.; Matsuda, K.; Konishi, T. *Kobunshi Ronbunshu* **1998**, *55*, 277.
(15) Wienk, M.; Struijk, M.; Janssen, R. *Chem. Phys. Lett.* **2006**, *422*, 488.
(16) Bongiovanni, G.; Loi, M. A.; Mura, A.; Piaggi, A.; Luzzati, S.; Catellani, M. *Chem. Phys. Lett.* **1998**, *288*, 749.
(17) Jespersen, K. G.; Beenken, W. J.; Zaushitsyn, Y.; Yartsev, A.; Andersson, M.; Pullerits, T.; Sundström, V. *J. Chem. Phys.* **2004**, *121*, 12613.
(18) Bredas, J. L.; Themans, B.; Andre, J. M.; Heeger, A. J.; Wudl, F. *Synth. Met.* **1985**, *11*, 343.
(19) Hoogmartens, I.; Adriaensens, P.; Vanderzande, D.; Gelan, J.; Quattrocchi, C.; Lazzaroni, R.; Bredas, J. L. *Macromolecules.* **1992**, *25*, 7347.
(20) Petersen, M. H.; Hagemann, O.; Nielsen, K. T.; Jorgensen, M.; Krebs, F. C. *Sol. Energy Mater. Sol. Cells* **2007**, *91*, 996.
(21) Karsten, B. P.; Viani, L.; Gierschner, J.; Cornil, J.; Janssen, R. A. *J. Phys. Chem. A* **2009**, *113*, 10343.
(22) Zoombelt, A. P.; Fonrodona, M.; Turbiez, M. G. R.; Wienk, M. M.; Janssen, R. A. J. *J. Mater. Chem.* **2009**, *19*, 5336.
(23) Zoombelt, A. P.; Leenen, M. A. M.; Fonrodona, M.; Nicolas, Y.; Wienk, M. M.; Janssen, R. A. J. *Polymer.* **2009**, *50*, 4564.
(24) Zoombelt, A. P.; Gilot, J.; Wienk, M. A.; Janssen, R. A. J. *Chem. Mater.* **2009**, *21*, 1663.
(25) Pomerantz, M.; Gu, X. M.; Zhang, S. X. *Macromolecules.* **2001**, *34*, 1817.
(26) Sotzing, G. A.; Lee, K. H. *Macromolecules.* **2002**, *35*, 7281.
(27) Liang, Y.; Xu, Z.; Xia, J.; Tsai, S.-T.; Wu, Y.; Li, G.; Ray, C.; Yu, L. *Adv. Mater.* **2010**, *9999*, NA.
(28) Liang, Y. Y.; Wu, Y.; Feng, D. Q.; Tsai, S. T.; Son, H. J.; Li, G.; Yu, L. P. *J. Am. Chem. Soc.* **2009**, *131*, 56.
(29) Chen, H. Y.; Hou, J. H.; Zhang, S. Q.; Liang, Y. Y.; Yang, G. W.; Yang, Y.; Yu, L. P.; Wu, Y.; Li, G. *Nat. Photonics* **2009**, *3*, 649.
(30) Liang, Y. Y.; Feng, D. Q.; Wu, Y.; Tsai, S. T.; Li, G.; Ray, C.; Yu, L. P. *J. Am. Chem. Soc.* **2009**, *131*, 7792.
(31) Liang, Y.; Xiao, S.; Feng, D.; Yu, L. *J. Phys. Chem. C* **2008**, *112*, 7866.
(32) Liang, V. Y.; Feng, D. Q.; Guo, J. C.; Szarko, J. M.; Ray, C.; Chen, L. X.; Yu, L. P. *Macromolecules.* **2009**, *42*, 1091.
(33) Szarko, J.; Guo, J. C.; Liang, Y. Y.; Rolczynski, B.; Yu, L. P.; Chen, L. X. *Proc. SPIE* **2008**, *7034*, 3403.
(34) Becker, R. S.; de Melo, J. S.; Macanita, A. L.; Elisei, F. *Pure. Appl. Chem.* **1995**, *67*, 9.
(35) Becker, R. S.; de Melo, J. S.; Macanita, A. L.; Elisei, F. *J. Phys. Chem. C* **1996**, *100*, 18683.
(36) Beljonne, D.; Shuai, Z.; Bredas, J. L. *J. Chem. Phys.* **1993**, *98*, 8819.
(37) Beljonne, D.; Cornil, J.; Friend, R. H.; Janssen, R. A. J.; Bredas, J. L. *J. Am. Chem. Soc.* **1996**, *118*, 6453.
(38) Colditz, R.; Grebner, D.; Helbig, M.; Rentsch, S. *Chem. Phys.* **1995**, *201*, 309.
(39) Cornil, J.; Beljonne, D.; Bredas, J. L. *J. Chem. Phys.* **1995**, *103*, 842.
(40) Hong, S. Y.; Marynick, D. S. *Macromolecules.* **1992**, *25*, 4652.
(41) Moet, D. J. D.; Koster, L. J. A.; de Boer, B.; Blom, P. W. M. *Chem. Mater.* **2007**, *19*, 5856.
(42) Zou, J. H.; Khondaker, S. I.; Huo, Q.; Zhai, L. *Adv. Funct. Mater.* **2009**, *19*, 479.
(43) Lee, B.; Seshadri, V.; Palko, H.; Sotzing, G. A. *Adv. Mater.* **2005**, *17*, 1792.
(44) Janssen, R. A. J.; Smilowitz, L.; Sariciftci, N. S.; Moses, D. *J. Chem. Phys.* **1994**, *101*, 1787.
(45) DiCesare, N.; Belletete, M.; Garcia, E. R.; Leclerc, M.; Durocher, G. *J. Phys. Chem. A* **1999**, *103*, 3864.
(46) Lanzani, G.; Nisoli, M.; Desilvestri, S.; Tubino, R. *Chem. Phys. Lett.* **1996**, *251*, 339.

(47) Yang, A.; Kuroda, M.; Shiraishi, Y.; Kobayashi, T. *J. Phys. Chem. B* **1998**, *102*, 3706.
(48) Wells, N. P.; Boudouris, B. W.; Hillmyer, M. A.; Blank, D. A. *J. Phys. Chem. C* **2007**, *111*, 15404.
(49) Westenhoff, S.; Daniel, C.; Friend, R. H.; Silva, C.; Sundstrom, V.; Yartsev, A. *J. Chem. Phys.* **2005**, *122*, 094903.
(50) Shaw, P. E.; Ruseckas, A.; Samuel, I. D. W. *Adv. Mater.* **2008**, *20*, 3516.
(51) Goh, C.; Scully, S. R.; McGehee, M. D. *J. Appl. Phys.* **2007**, *101*, 114503.
(52) Meier, H.; Stalmach, U.; Kolshorn, H. *Acta Polym.* **1997**, *48*, 379.
(53) Yao, Y.; Liang, Y.; Shrotriya, V.; Xiao, S.; Yu, L.; Yang, Y. *Adv. Mater.* **2007**, *19*, 3979.
(54) Izumi, T.; Kobashi, S.; Takimiya, K.; Aso, Y.; Otsubo, T. *J. Am. Chem. Soc.* **2003**, *125*, 5286.
(55) Wang, Z.; Kobayashi, T. *New. J. Phys.* **2008**, *10*, 123021.
(56) Hammond, V. J.; Price, W. C. *Trans. Faraday. Soc.* **1955**, *51*, 605.
(57) Bednarz, M.; Reineker, P.; Menaosteritz, E.; Bauerle, P. *J. Lumin.* **2004**, *110*, 225.
(58) Chen, L. X.; Jager, W. J. H.; Niemczyk, M. P.; Wasielewski, M. R. *J. Phys. Chem. A* **1999**, *103*, 4341.
(59) Thompson, B. C.; Frechet, J. M. J. *Angew. Chem., Int. Ed.* **2008**, *47*, 58.

JP101925B